https://dx.doi.org/10.1016/j.cemconcomp.2018.02.010

Citation: Jian-Xin Lu, Chi Sun Poon, Improvement of early-age properties for glass-cement mortar by adding nanosilica, Cement and Concrete Composites 89 (2018) 18e30. https://doi.org/10.1016/j.cemconcomp.2018.02.010

Improvement of early-age properties for glass-cement mortar by adding nanosilica

Jian-Xin Lu [a,b], Chi Sun Poon [a,*]

[a] Department of Civil and Environmental Engineering, The Hong Kong Polytechnic University, Hung Hom, Kowloon, Hong Kong

[b] Construction and Building Materials Research Center, Nano and Advanced Materials Institute Limited, Hong Kong Science Park, Shatin, Hong Kong

*Corresponding author: cecspoon@polyu.edu.hk

Abstract:

Poor early-age performance (e.g. lower early strength, longer setting time) is an important technical challenge for the application of blended cementitious materials containing low reactivity or high volumes of supplementary cementing materials. In this study, the mechanism of using nanosilica (NS) to improve the early-age properties for cement mortars blended with glass powder (GP) and glass aggregates has been investigated. The results indicate that the addition of NS into glass-based cement mortar largely improved the early stiffening which was dependent on high specify surface area of the NS rather than cement hydration. Combining the use of NS and GP was conducive to compensate the delayed setting times and the strength losses caused by the incorporation of GP. These beneficial behaviors were associated with the physical, acceleration, pozzolanic and pore refinement effects of NS. In terms of heat of hydration, the inclusion of NS intensified and accelerated the appearance of the third exothermic peak (AFt to AFm) due to the absorption of sulfate ions by the increased C-S-H formation. Also, the total hydration heat liberated was found to correlate linearly with the corresponding early-age compressive strength. Microstructural analysis suggest that NS significantly helped to densify the microstructure of the GP blended cement matrix and improved the interface between the GP particle and the binder matrix. This was verified by the contribution of NS on refining the coarse pore size caused by the use of GP as a replacement of cement.

Keywords: Nanosilica; Waste glass; Glass powder; Early-age properties; Cement mortar

1 Introduction

1.1 Background

Soda-lime-silica glass has been widely used for producing beverage containers due to its chemical stability [1]. On the other hand, the management of the post-consumer beverage glass bottles has become an urban waste issue. In Hong Kong, there were nearly 275 tones waste glass bottles being generated per day in 2015 [2]. However, it is not easy to establish waste glass recycling industries when land is scarce and costly, especially for handling the waste glass with lower recyclable value. Currently, less than 10% of the waste glass was recycled in Hong Kong, that is to say, more than 90% of waste glass has to be disposed at landfills. But according to estimation of the government, the three large, modern state-of-the-art landfills built will reach their designed capacities one-by-one by 2019 [3]. Therefore, waste glass recycling is an important element of the local waste management framework, which not only help to conserve natural resources but also reduce demand for valuable landfill space.

Recycling waste glass for the production of cement-based construction materials has attracted a lot of interests in the past few years [4-19]. The main forms of waste glass employed in concrete or mortars were glass cullet as fine aggregates [4,5] and glass powder as a supplementary cementitious material (SCM) [6-16]. A comprehensive experimental programme including studying the fresh, mechanical and durability properties of concrete or mortars incorporating waste glass has been conducted. Furthermore, to maximize the utilization of waste glass, several researchers simultaneously used glass aggregates and glass powder in concrete [17,20] or mortars [19]. Based on the experimental and field results, it is possible to use waste glass in the production of cement-based construction products in either aggregates form or powder forms.

Recently, the research group in the Hong Kong Polytechnic University developed a novel recycled glass architectural mortar, which could fully utilize the aesthetic nature of waste glass [21,22]. The waste glass is used as decorative aggregates not only making use of the appealing colors of the mixed glass cullet but also reducing virgin aggregates consumption. In addition, the potential applications of recovered glass materials in architectural mortars could diversify the recycling outlets and relieve environmental stresses on landfill disposal.

As for the performance of concrete or mortar incorporating glass aggregates (GA) to replace natural aggregates, there are many advantages. The inclusion of GA contributed to increasing the workability of the concrete [4] and mortars [5] due to the smooth surface texture of the glass. Also, since the GA had lower water absorption values, the transport properties of the concrete were improved as the GA content increased [4]. Meanwhile, the increase in GA content led to a reduction in drying shrinkage of the concrete [23] and mortars [5,24]. The addition of GA into the concrete also could effectively improve the resistance to chloride ion penetration [23,24] and sulfate attack [21,25]. Furthermore, increasing the content of GA in the mortar produced a gradually beneficial effect on the residual compressive strength and elastic modulus after the mortar was exposed to 800 °C [26].

However, several detrimental effects were also incurred by using glass cullet as aggregates. The substitution of the fine aggregates by the GA resulted in reductions in the compressive, flexural, splitting tensile strengths and elastic modulus of the concrete because of the weaker ITZ between the GA and the matrix [4,5,17,24]. Even worse, the alkali-silica-reaction (ASR) induced by the GA was the major obstacle for its application in cement-based systems [5,27]. Our recent works have proven that the use of the different SCMs could improve the mechanical and durability performance of the architectural mortars containing 100% GA [19,28]. In particular, combining the use of waste glass powder (GP) was able to overcome the drawbacks resulting from the incorporation of GA (i.e. reduced strength and ASR expansion). This encouraging result provided an effective way for maximizing the use of waste glass in cement mortars. However, compared to other SCMs, the GP has a lower reactivity [28], which is in particular detrimental to the early-age properties. Indeed, the previous results showed that the early strengths were significantly reduced [19] and the setting times were also delayed [18] as the GP was introduced to replace the cement. Therefore, there is a need to improve the early-age properties of the architectural cement mortar with a view to enhancing the production efficiency.

Recently, nanosilica (NS) has been successfully used in fly ash–concrete/mortars to improve the mechanical properties at early stages [29-31]. Hence, it is expected the use of NS can counteract the undesirable early-age properties of the glass-based cement mortars. Previously, a limited number of investigations had been carried out to study the effect of a hybrid combination of NS and waste glass on the properties of concrete or mortars [32,33]. But, few studies have been done with respect to the early-age properties of cement mortars containing NS and waste glass. Thus, this work aimed to using NS to improve the early-age properties of the cement mortar prepared with GA as fine aggregates and GP as a cement replacing material. In addition, a novel calender extrusion method is designed to produce the glass-based architectural cement mortar with a view to enhancing the production efficiency (see Fig. 1), considering the processing requirement for the architectural cement mortar, related properties including workability, stiffening time, setting time and early strength were investigated. Furthermore, the corresponding heat of hydration and microstructure (SEM, TG, MIP) analyses were also determined to understand the roles of NS in the glass-based cement mortar.

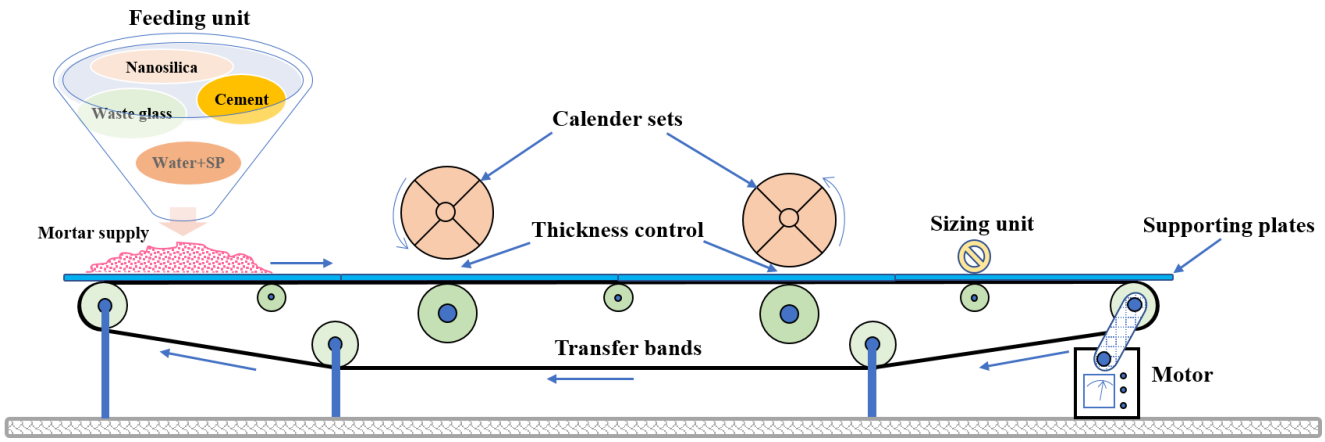

Fig. 1 Calender extrusion method in the production of recycled glass architectural mortar

1.2 Research significance

Generally, SCMs are understood to increase the long-term strength of cementitious materials through the pozzolanic reaction while decrease early-age strength due to the dilution effect (i.e. less Portland cement). This is of particular concern when attempting to replace cement with high volumes of SCMs. Therefore, one of the challenges that arise from increasing the use of SCMs or incorporating SCMs with very low reactivity (such as GP) is to improve the early-age properties of such blended materials. In this study, NS was employed into the GP-containing pastes/mortars to optimize the early age properties the cementitious materials.

2 Materials and experimental methodology

2.1 Materials

2.1.1 Cement and Glass powder (GP)

For purpose of producing architectural mortar with aesthetic appearance, a white ordinary Portland cement manufactured by PT. Indocement Tunggal Prakarsa Tbk in Indonesia was used for this experiment. This white cement (WC) type was CEM I (52.5N), conforming to BS EN 197-1. GP was obtained by grinding waste glass cullet (see 2.1.3 section) with a laboratory ball mill for 1 hour. The compositions and particle size distributions of the WC and GP are presented in Table 1 and Fig. 2, respectively. The corresponding mean diameters of the WC and GP were 14.1 μm and 99.3 μm, which indicates that the fineness of WC was much higher than that of GP.

Table 1

Compositions of WC and GP (ms %).

	Compositions	WC	GP
Chemical composition	SiO_2	20.41	73.5
	Al_2O_3	4.88	0.73
	Fe_2O_3	0.35	0.38
	CaO	68.21	10.48
	MgO	1.73	1.25
	K_2O	0.25	0.69
	Na_2O	-	12.74
	TiO_2	-	0.087
	SO_3	3.58	-
	P_2O_5	0.087	-
	SrO	0.4	-
	Cr_2O_3	0.041	-
Mineral phases	C_3S	51.32	-
	C_2S	27.14	-
	C_3A	12.94	-
	C_4AF	1.07	-

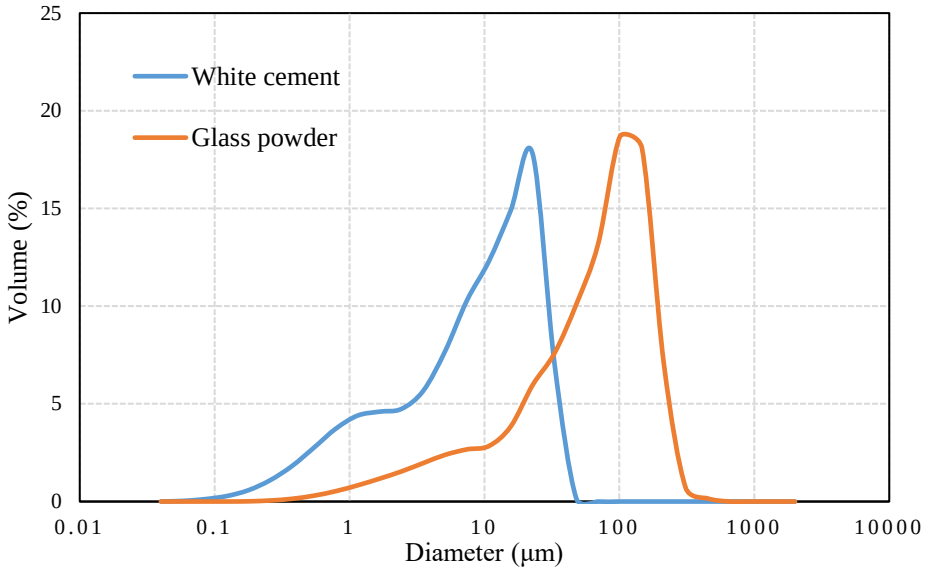

Fig. 2 Particle size distributions of WC and GP

2.1.2 Nanosilica (NS)

A commercial NS (VK-SP30) supplied by Xuancheng Jingrui New Materials Co., Ltd. (Anhui, China) was used. The information of the NS provided by the supplier is listed in Table 2. Also, the morphologies of the NS obtained from transmission electron microscopy (TEM, JEOL JEM-2011) are shown in Fig. 3. It can be seen that the NS particles were extremely fine with particle size of about 30 nm and had very high surface area. It is clear that serious agglomeration of the NS particles was observed without effective dispersion.

Table 2

Physiochemical properties of powdered NS.

Properties	Characteristics
Appearance	White powder
Silica content	99.8%
Diameter	30±5 nm
Specific surface area	220±30 m^2/g
pH value	5-7

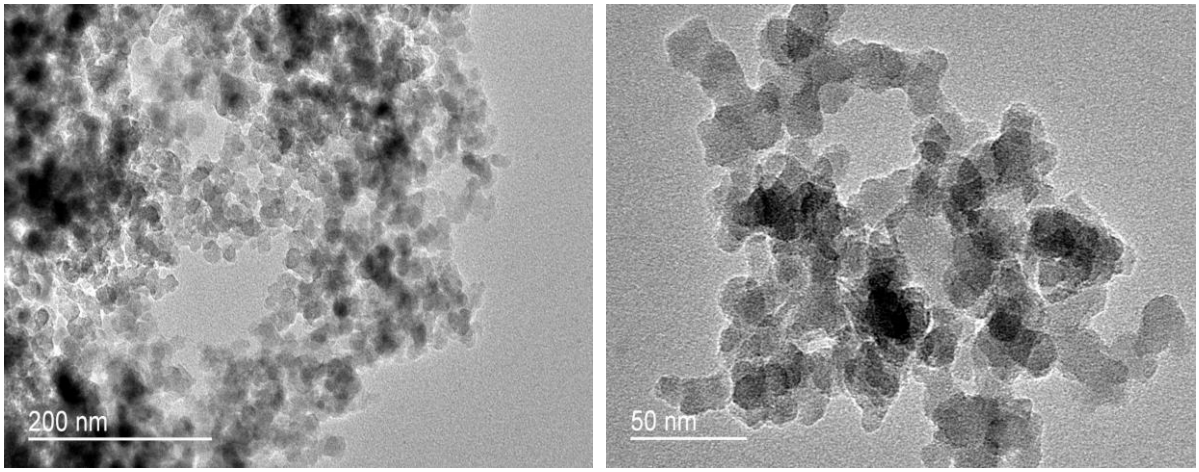

(a) TEM image at 200 nm scale (b) TEM image at 50 nm scale

Fig. 3 Morphologies of NS

2.1.3 Recycled glass cullet (RGC)

The fine aggregates used in this study was RGC with a fineness modulus of 3.21, which was collected from a waste glass recycler in Hong Kong. This RGC was a mixed glass derived from crushing post-consumer beverage bottles. Before using the RGC into the architectural mortar, the glass cullet was rinsed with tap water first to remove most of the contaminants (e.g. paper and plastics), and then oven-dried for a minimum of 24 hours at 105 °C. The appearance and gradation curve of RGC are presented in Fig. 4.

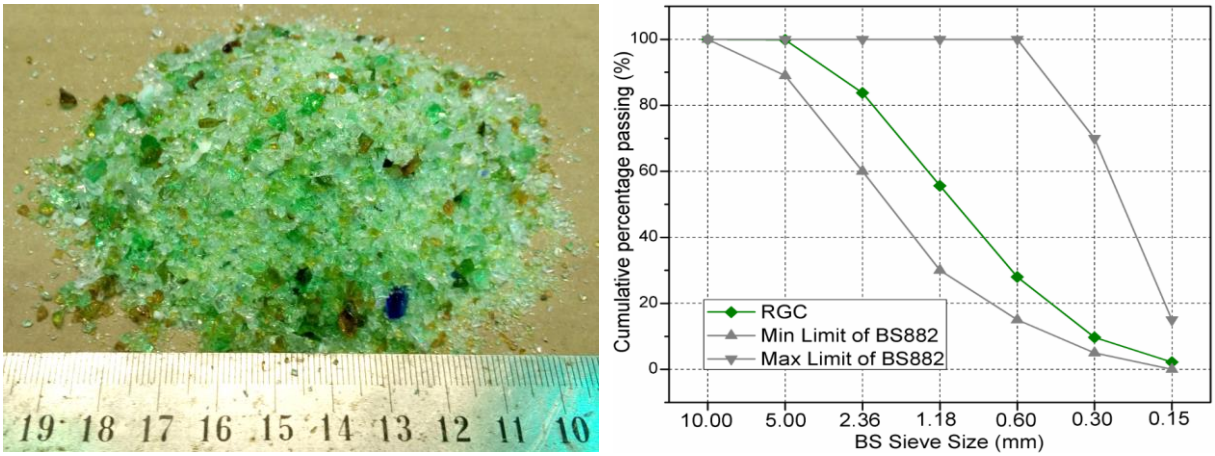

(a) Appearance of RGC (b) Gradation curve of RGC

Fig. 4 Characteristics of RGC

147
148

149 **2.2 Mixture proportioning and specimen preparation**

150 In order to fulfill the aesthetic requirement and enhance the recycling rate of waste glass in Hong Kong, the
151 fine aggregates in the architectural mortar were fully replaced by RGC. Moreover, GP obtained from RGC
152 was used to further replace 20% of the WC. A polycarboxylate based superplasticizer (SP) with the
153 commercial name ADVA-109 (W.R. Grace) was used to improve the workability and served as the
154 dispersant of NS powder into water. The mixture proportions, incorporating different mass fractions of NS,
155 are given in Table 3. A constant water-to-binder ratio of 0.4 was used for all the mixtures. The
156 binder-to-aggregate ratio was chosen to be 0.5. The dosages of the additional NS varied from 0 to 0.5%,
157 1.0%, 1.5% and 2.0% by mass of the cementitious materials calculated based on the binder content of the
158 mix (by weight).

159

160 Table 3

161 Mix proportions for glass-based architectural mortars.

Mix	NS	WC (kg/m^3)	GP (kg/m^3)	RGC (kg/m^3)	NS (kg/m^3)	Water (kg/m^3)	SP (kg/m^3)
CON	0	706	0	1412	0	283	5.65
GP	0	565	141	1412	0	283	5.65
GP-0.5NS	0.5%	565	141	1412	3.53	283	5.65
GP-1NS	1.0%	565	141	1412	7.06	283	5.65
GP-1.5NS	1.5%	565	141	1412	10.59	283	5.65
GP-2NS	2.0%	565	141	1412	14.12	283	5.65

162 Note: The numbers in the mix designation correspond to the presence of GP and percentage of NS present
163 in the binder. For example, the sample GP-2NS means that the cement mortar was prepared with 20% GP
164 and 2% NS. CON stands for the control mix with 100% WC.

Mixing of the cement mortar mixtures was conducted in a mortar mixer (FARGO, CE-212XG). In the procedure of mortar preparation, the required water and SP were first mixed well together first. For better dispersion of NS within the glass mortar (if any), the weighed NS was added to the mixed solution of water and SP, followed by two minutes mixing in the mortar mixer at a speed of 121 rpm. On the other hand, the WC, GP (if any) and RCG were weighed according to the stipulated proportion and mixed thoroughly in separately in another mixer. Afterwards, these dry materials (WC-GP-RCG) were introduced to the NS-water-SP mix and then mixing was carried out for three more minutes at three different speeds (first minute at a speed of 121 rpm, second minute at a speed of 218 rpm, third minute at a speed of 489 rpm), respectively. Finally, the fresh mortars were casted in moulds or used for each test as described in the following sections.

2.3 Test methods

2.3.1 Workability

Once the mortar mixture was ready, the slump flow was measured by a spread flow cone according to BS EN1015 [34]. The fresh mixture was filled into a mini-slump cone with 100 mm internal diameter on a 250 mm flow table disc. Then, the conic mould was slowly raised vertically to spread out the fresh mixture on the disc. The spread diameters of the fresh mixture after jolting the flow table 15 times were measured from 5 to 30 min at intervals of 5 mins. The measurement time started from the moment of contact between the water and the cement. After testing one batch, the mixture in the mould was discarded and a new mixture was taken out from the mixer bowl for another flow test.

2.3.2 Stiffening

This test was performed to determine the degree of the early stiffening of the cement mortars with the incorporation of NS. The preparation of cement mortars was mentioned in section 2.2 and the test method was conducted according to ASTM C359 [35]. After completion of mixing, a portion of ready-mixed mortar was immediately cast into a plastic container (50 × 50 × 150 mm) until the container was heaping full. A modified Vicat apparatus was used to measure the penetration of a plunger at 5 min, 8 min, 11 min, 15 min, 20 min, 25 min, and 30 min after the beginning of mixing between the water and the mortar. Every test value recorded was the average of two measurements.

2.3.3 Setting time

The setting time of cement pastes with and without NS was evaluated in accordance with BS EN 196-3: 2005+Al: 2008 [36]. The *w*/*b* of the pastes was set to 0.4 in order to be comparable with that of the mortars.

2.3.4 Compressive strength

The fresh mortars were cast in steel cubic moulds (50 × 50 × 50 mm) in two approximately equal layers, each layer was compacted on a vibrating table for 15s. A plastic film was used to cover the surface of mortars to avoid the evaporation of moisture. After nearly 24 h, the specimens were demoulded from the moulds. Immediately, three specimens of each mix were used to test the one-day compressive strength using a compression machine with maximum capacity of 300 kN. The loading rate was controlled at 0.6 kN/s during the test. Another three specimens were cured in a water tank at 23±2 °C until the age of 3 days. Then, the specimens were removed from the tank and the 3-day compressive strength of mortars was measured in the same way.

2.3.5 Heat of hydration

An isothermal calorimeter (Calmetrix I-CAL) was used to determine the heat evolution during hydration. The cement pastes were prepared using the proportion in Table 3, but without the addition of RGC. Measurement in this study was carried out under an isothermal condition (20 ºC) and the heat flow was recorded for 3 days.

2.3.6 Microstructure analyses

After testing the setting time, the pastes used were stored in a sealed plastic bag until 24-hour. A portion of hardening paste was broken into small fragments with diameters of 4-6 mm and soaked in ethanol to stop further hydration. The rest of the paste was transferred into a water tank at 23±2 °C to cure for another 2 days. Similarly, small fractured specimens were obtained from the 3 day cured pastes and their hydration was also stopped by solvent exchange using ethanol.

After immersion in ethanol for 3 days, the samples were dried at 60 °C in a vacuum drying oven for 48 hours to remove the residual ethanol. Then, the prepared samples were used for analyzing the microstructure by means of Scanning Electron Microscopy (SEM) and Mercury Intrusion Porosimetry (MIP). Morphological observations analysis was performed on gold-coated samples using a SEM (Tescan VEGA3). MIP (Micromeritics AutoPore IV 9500 Series) with a maximum mercury intrusion pressure of 207 MPa was employed for determining the porosity and the pore size distributions of the pastes. The porosity measured by this method was a wide range of pore sizes from 150 μm down to 7 nm. This test used the usual assumption that the pores were cylindrical and the contact angle was taken as 140°. Although the MIP method may not exactly reflect the true porosity of the cement-based materials (necking effect) and the drying condition is also known to modify the porosity, MIP is also thought to be a simple and reliable technique for quantitatively and qualitatively comparing pore structures between different cementitious materials [37]. Thermal gravimetric (TG) analysis technique was adopted to measure the free calcium hydroxide (CH) content in the pastes by using a Rigaku instrument (Thermo Plus Evo2 8121). The broken

pieces of pastes were ground into powder with particle sizes smaller than 75 μm. Approximately 10 mg powdered sample was placed in a ceramic crucible for heating. The samples were heated under atmosphere in the furnace, where the temperature was programmed to rise at a constant heating rate of 10 °C/min up to 1000 °C. After completing the test, the quantity of CH was determined from both the dehydroxylation (WL_{CH}) and decarbonation (WL_{CaCO3}) losses from the mass loss data. The calculation equation is given by sum of WL_{CH} and WL_{CaCO3} losses as below [38]. The CH content result reported was an average of two measurements.

$$\text{CH content (\%)} = 4.11WL_{CH}+1.68WL_{CaCO3} \quad (1)$$

Where

WL_{CH} is the weight loss during dehydroxylation (between 400 °C and 500 °C)

WL_{CaCO3} is the weight loss during decarbonation (between 600 °C and 750 °C)

3 Results and discussion

3.1 Workability

Fig. 5 shows the effect of NS on the flow values of the recycled glass cement mortars prepared with GP. The flow values decreased with time, which was related to the hydration of the cement (to be discussed in section 4.1). Regardless of the testing time, the control mortar always had the highest flow values. However, the replacement of cement by GP resulted in a slight reduction in workability. This may be due to the fact that the irregular shape and bigger particle size of GP hindered the movement of the mortar [18]. It is apparent that the addition of NS brought about a dramatic drop in the flow values even if 0.5% NS was added into the mix. As shown in Fig. 3, the NS has very high surface area and extremely fine particle size. This indicates that a large amount of water was required to coat the fine NS particles. Therefore, the flow values of the cement mortar were reduced significantly as the dosage of NS increased. For the mortar prepared with GP alone, a little influence on the workability of cement mortar was observed. The reason is that the particle size of the GP was close to that of cement particle as compared to the extremely fine particle size of NS.

It should be noted that the severe workability loss because of NS addition is a drawback for conventional cement mortar. But in this study, a calender extrusion method as mentioned will be applied for producing the glass-based architectural mortar. Hence, a low but adequate workability (i.e. semi-flow under specific pressure) of the fresh cement mortar is needed to keep the shape of mortar after casting. From the workability results, a moderate amount of NS addition was helpful to provide an extrudable mixture.

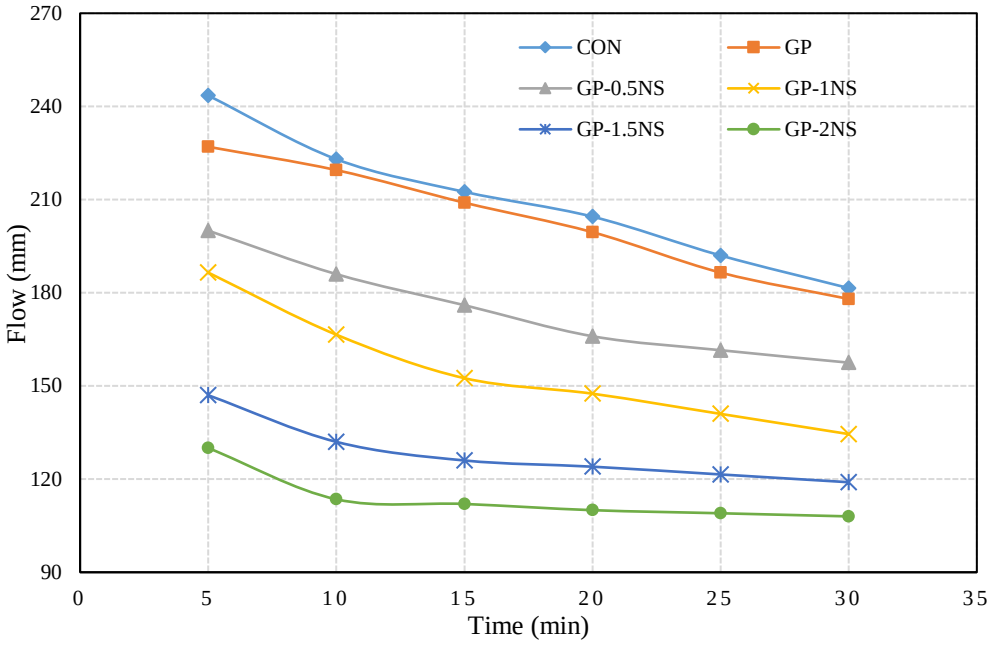

Fig. 5 Flow of the cement mortars containing GP and NS

3.2 Early stiffening

The early stiffening test was used to assess the rheological behavior of fresh glass mortar prepared with GP and NS. The testing results for cement mortars containing GP and different NS contents are shown in Fig. 6. Obviously, reductions in the penetration depth over time were observed, which were mainly associated with the hydration of cement. As the hydration progressed, the cement minerals reacted with water to form the hydration products which produced a solidified mass. It can be seen that the use of GP as a cement replacement led to an increase in the stiffening rate of the mortar. A possible explanation is that the larger particle size and irregular shape of GP provided interlocking between the particles, thus increased the resistance to penetration [18]. In the cases of GP mortar without and with NS, a significant difference occurred in the stiffening rate. When 0.5% NS was added into the GP mortar, a slight decrease in the penetration was noticed. Nevertheless, a further NS content increased to 1% NS in the GP mortar induced a strong resistance to the penetration, indicating that the mortar modified with 1% NS had a rapid stiffening ability. Furthermore, as the dosage of NS was increased to 1.5% and 2%, there were dramatic reductions in the penetration depth, which reveals that the inclusion of NS could greatly enhance the stiffening rate of the GP mortar.

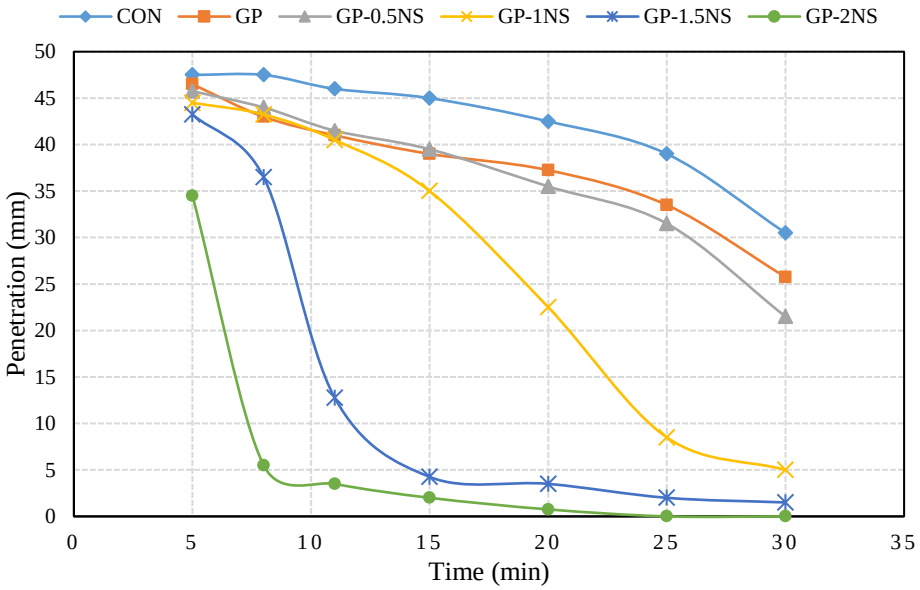

Fig. 6 Stiffening of cement mortars containing GP and NS

The primary sources of such enhancement of stiffening by the addition of NS might be related to two factors: cement hydration and specific surface area of NS. For hydration, the stiffening was tested within 30 min after mixing with water which was before the end of the dormant period. This is consistent with the fact that during the initial hydration process, the total heat evolved was very low. This indicates that the hydration during this early age had only a small contribution to the early stiffening. It should further be noticed that the pure cement paste developed a comparable heat output to the GP paste with 1% NS (see Fig. 9a) while the stiffening rate of the pure cement paste was well slower than the GP mortar with 1% NS. Such behavior further confirmed that the enhancement of the stiffening was not controlled by the effect of NS on the cement hydration. As indicated by the results of workability, the NS with very fine particle size largely influenced the flow values. Similarly, the NS with a huge specific surface area could induce much higher viscosity of the cement mortar due to the consumption of large amount of free water. Moreover, the fine NS particles would also fill in the void between the grains, resulting in a dense packing matrix. Thus, the resistance to the penetration by NS modified mortar causing early stiffening within the first 30 min was highly dependent on specific surface area of the NS. Based on this theory, due to the relatively similar specific surface area of GP and WC, the stiffening property of GP blended mortar was similar to that of control mortar.

3.3 Setting time

The setting times of the GP blended cement pastes with and without NS addition are illustrated in Fig. 7. It is found that replacing 20% cement by GP delayed the initial and final setting times of the cement paste by around 23% and 20%, respectively. This behavior was mainly attributed to the low reactivity of GP with a

larger particle size. Moreover, the non-absorbent nature of the glass particles induced an increase of the effective water-to-cement (*w*/*c*) ratio in the paste, making it to take a longer time to form a rigid structure [39]. Obviously, the addition of NS was conducive to shortening the setting times. Moreover, the initial and final setting times decreased significantly as the dosage of NS increased. When 1.5% NS was added into the GP blended cement paste, the setting times were similar to the control cement paste, which means that the introduction of a small quantity of NS (1.5%) in GP paste could make up the extension of setting times resulted from the replacement of cement by GP in the paste. Furthermore, with the incorporation of 2% NS, the initial and final setting times were reduced by 29% and 24%, respectively, in comparison to that of the cement paste prepared with GP alone. The reduction of the setting times of the NS modified pastes containing GP may be caused by the finer particle size and higher surface area of the NS, which may accelerate the cement hydration by providing a large amount of nucleation sites for precipitation of cement hydration products [40]. This phenomenon is in accordance with the findings of Zhang and Islam [30], who reported that the incorporation of 2% NS could largely reduce initial and final setting times of concrete prepared with high-volume fly ash or slag.

Another interesting observation is that the setting times shortened with the addition of NS were mainly attributed to the shortening of the initial setting. This result is consistent with the work of Chen et al. [41]. Generally, the initial setting of cement occurs in the acceleration period of hydration, where the tricalcium silicate (C_3S) hydrates rapidly to form the calcium silicate hydrate (C-S-H) phase and CH. Furthermore, the findings reported by Land and Stephan [42] showed that the incorporation of NS contributed to faster consumption of C_3S and faster formation of CH. Thereby it is inferred that the reaction of the acceleration period was speeded up by the addition of NS (to be confirmed by heat of hydration results). Then, setting would be brought forward as more hydration products of individual grains formed came into contact with one another.

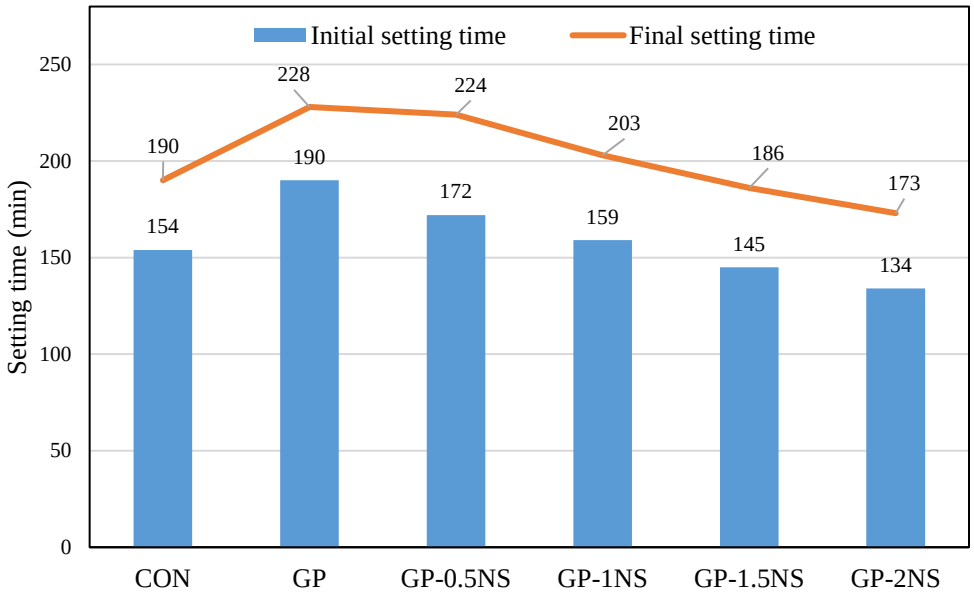

Fig. 7 Setting time of cement pastes containing GP and NS

3.4 Early-age compressive strength

The influence of NS on the early-age compressive strength (1 day and 3 days) of the GP blended mortar is demonstrated in Fig. 8. The control mortar was also chosen as a reference. Apparently, it can be seen that the replacement of cement by GP led to dramatic drops in the early compressive strength. The reason is that the GP with larger particle size had a low reactivity at the early ages. Moreover, the higher effective *w*/*c* ratio due to the non-absorbent nature of GP may further reduce the early-age strength of the cement mortar. However, it is obvious that the addition of NS could significantly increase the early compressive strength of the mortar containing GP. Also, in spite of the ages, the strength was raised gradually as the NS content increased. An encouraging result should be noticed is that, after 3 days of curing, the inclusion of 2% NS in the GP blended mortar achieved a comparable compressive strength to that of the control mortar. Correspondingly, the strength of the GP mortar with 2% NS was increased by around 55% compared to that without NS. These results mean that the addition of NS can compensate the early strength losses of the mortar due to the incorporation of GP as a cement replacement. Similar results were also obtained by Zhang et al. [40], which found that with 1% NS (7 nm) addition, the compressive strengths of high-volume slag mortars were increased by 35% at 3 days in comparison to the reference concrete with 50% slag.

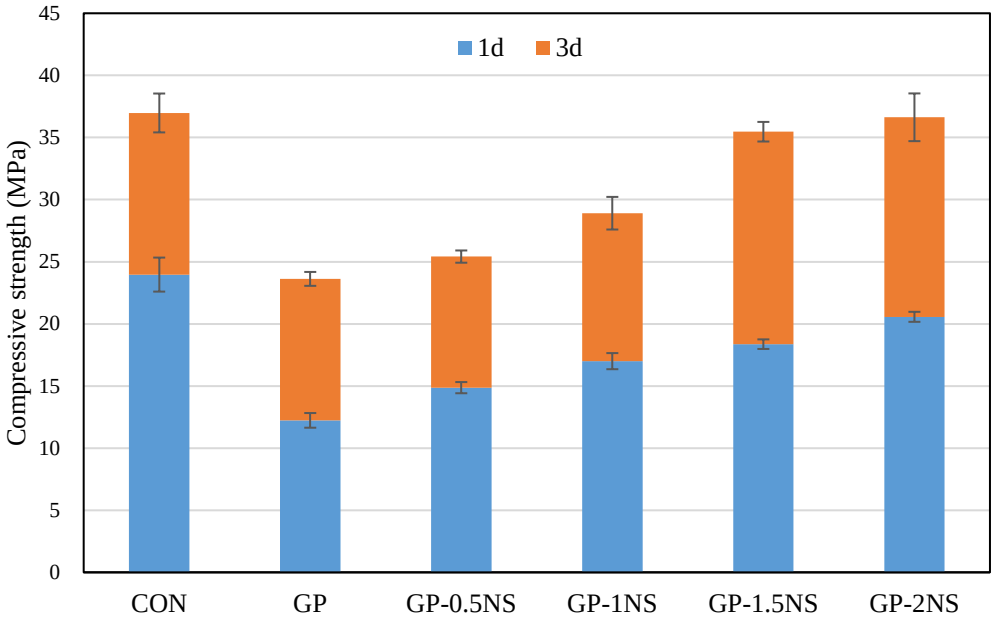

Fig. 8 Early-age compressive strength of cement mortars containing GP and NS

Several positive effects of NS on the early-age strength of GP blended mortar should be taken into consideration. (i) physical effect: the NS with ultra-fine particles would become a filler, which could fill up the voids between the cement grains and the GP particles. Hence, this might be helpful to strength enhancement due to the more effective packing and reduced porosity; (ii) acceleration effect: as mentioned before, the hydration of C_3S could be accelerated by the addition of NS, and the early formation of C–S–H would develop a higher strength at the early ages; (iii) pozzolanic effect: the NS with high pozzolanic reactivity could react with CH to produce additional C–S–H, which was the main contribution for the strength development of the hardened cement paste. At the same time, the CH generated during the hydration of cement, which only contributed slightly to the strength gain, was consumed (see section 4.3); (iv) pore refinement effect: based on the (iii) reaction, the formation of additional C-S-H and consumption of CH due to the pozzolanic reaction of NS would be conducive to produce a dense microstructure by refining the pore structure (see section 4.4).

4 Mechanism analyses from calorimetry, morphology, thermo-analysis and pore structure

4.1 Thermal calorimetry (Heat of hydration)

To understand the influence of the added NS on the hydration process of GP-WC blend, the hydration heat was recorded for a period up to 3 days. The evolution of hydration heat of the GP-WC pastes with different dosages of NS is shown in Fig. 9. Fig. 9a presents the rate of heat evolution, which is an indication of the rate of hydration. In general, the hydration process is classified into five principal stages, i.e. initial period, induction period, acceleration period, retardation period and steady period. The insert in Fig. 9a amplifies

the first peak, which corresponds to the initial period of hydration. During this stage, it is intuitively seen the occurrence of the first peak within a few minutes, which is referred to the superficial reaction of C_3S, tricalcium aluminate (C_3A) [43,44]. Hence, when the cement was replaced by the GP, the rate of heat flow decreased due to the dilution effect. However, it should be noted that the heat evolution rate increased with the increasing dosage of the NS in the GP blended paste. This indicates that the inclusion of NS promoted the hydration process although the hydration occurred just within the first few minutes. The acceleration effect of hydration caused by incorporating NS could also be partly responsible for the reduction in workability and early stiffening.

Following the induction stage with a low heat evolution rate, the rate of heat evolution increased significantly because of C-S-H gel nucleation and densification, as well as CH precipitation. It is worth noting that the addition of NS accelerated the heat evolution rate during the second peak. From the insert in Fig. 9b, the cumulative heat liberation profiles of the NS modified GP paste was also higher than that of the GP paste without NS added. These results are consistent with the results of setting time. The addition of NS could accelerate the hydration, thus shortened the setting time. During the nucleation and growth period, the NS particles might act as nuclei for the precipitation and growth of the initial hydration products, such as ettringite and C-S-H so that an increase of NS dosage expedited the progress of hydration.

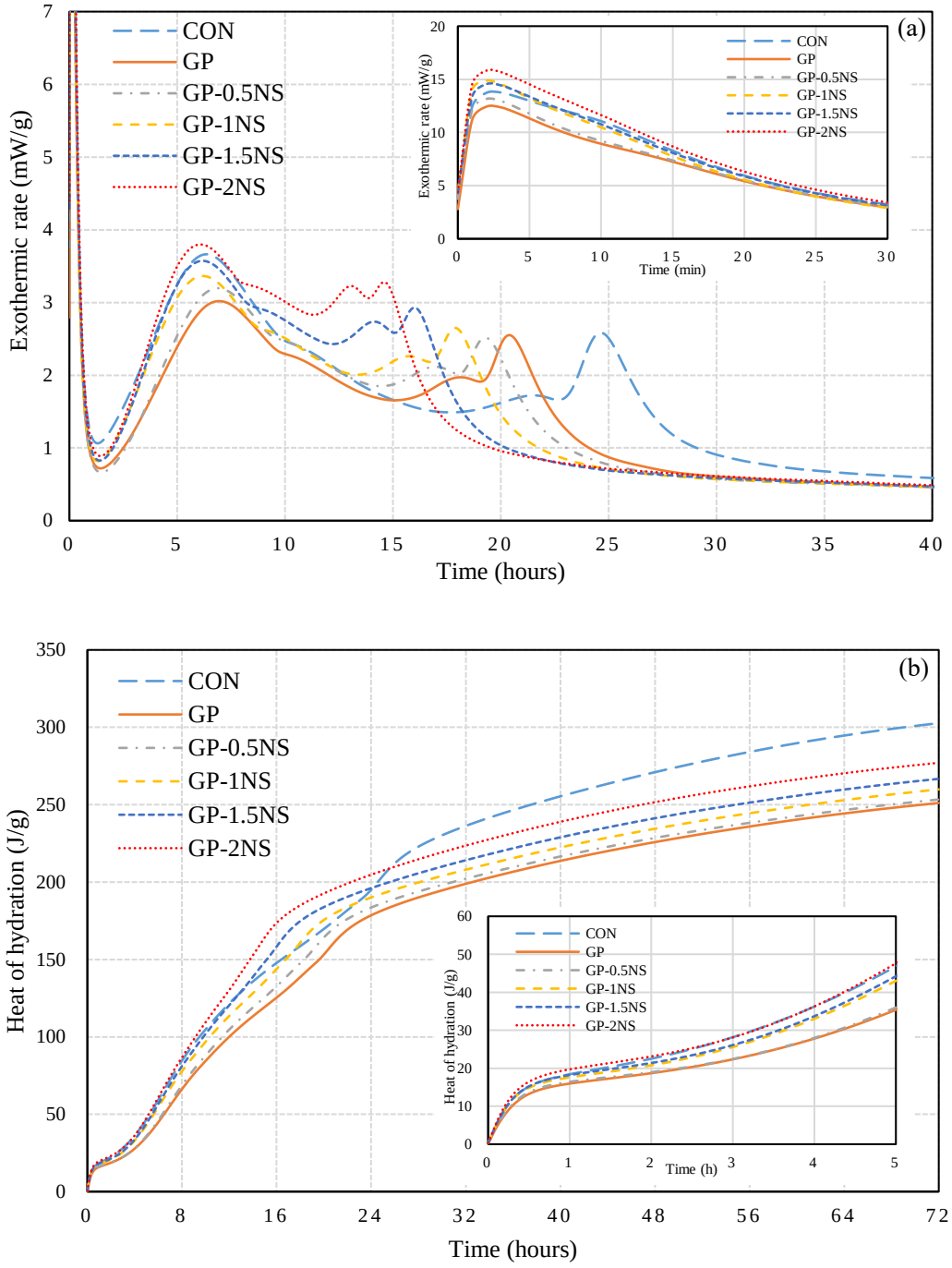

Fig. 9 Isothermal calorimetric curves for cement pastes containing GP and NS: (a) heat flow; (b) cumulative heat development

In particular, it should be noticed that an intense peak of heat evolution occurred in the shoulder of the curves after the maximum heat flow. Traditionally, the third exothermal peak is associated with the conversion of ettringite (AFt) into AFm phases [45]. Due to the higher C_3A content in the WC than the ordinary Portland cement, the heat evolution produced a broad and strong third peak [19]. A similar phenomenon was also observed in a previous study when the WC was used [42].

For the pure WC, the third peak appeared at approximately 25 hours after mixing. However, this peak shifted toward earlier time when part of the cement was replaced by the GP. This behavior can be explained by more water was available to accelerate the conversion reaction of AFt to AFm due to an increase in the effective *w*/*c* ratio induced by the replacement of cement by the GP [19]. When the NS was added in the GP blended paste, an apparent increase of heat output in the third peak was observed. Meanwhile, it can be observed that the larger the dosage of the NS, the earlier the formation of the AFm occurred. One possible reason proposed by Land and Stephan [42] was that the NS with a high surface area had a high capacity to adsorb sulphate ions, which resulted in a decrease of sulphate concentration and then caused an accelerated formation of the AFm.

On the other hand, according to the study of Quennoz and Scrivener [46], sulfate ions could be absorbed in the C-S-H. Moreover, the time of occurrence of the exothermic peak due to the aluminate reaction was directly affected by the amount of gypsum, and it was shifted to an earlier time with a decreasing gypsum content [47-49]. Meanwhile, the peak became higher and narrower as the gypsum content decreased [49] that is consistent with the hump trend in the calorimetric curve as the NS content increased. These findings provide a new explanation for the transference of the third exothermic peak in the case of the NS inclusions: the large increase in the second peak intensity indicated the more C-S-H formation due to the acceleration and pozzolanic effects of the NS. Hence, the third exothermic peak was possible to occur at an earlier time because of the absorption of sulfate ions by the large amount of C-S-H. In case of C_3A–gypsum systems, Quennoz and Scrivener [49] suggested that the acceleration part of this reaction was controlled by the surface area of the remaining C_3A where AFm phases nucleated. Based on this theory, the transference of the third peak was associated with two parameters: (i) when the NS was added in the paste, the sulfate could be absorbed by the large amount of C-S-H, which resulted in a lesser degree of reaction of C_3A. Thus, more remnant C_3A phases are available to react with AFt, that would lead to a higher conversion rate from AFt to AFm. (ii) Since the more C-S-H could absorb more sulfate, less ettringite was formed during the pre-peak period. Hence, more spaces were available for reactant growth during the reaction, this was helpful to the nucleation of AFm phases. However, it is uncommon to notice that a low and broad hump occurred before the distinct third-peak. A possible explanation may be the formation of delayed AFt due to the desorption of sulfate ions from C-S-H. Hence, as the content of NS increased, the shoulder peak became intense because more sulfate ions were released. But this hypothesis still needs further and more detailed studies.

Fig. 9b shows the cumulative total heat output of the cement pastes with and without incorporating GP and NS during 3 days. It can be seen that the heat output of the control specimen developed rapidly after 1 day. This is related to the conversion reaction of AFt to AFm happening at about 24-hour, which led to a relatively higher heat flow. However, the replacement of cement by the GP resulted in a reduction in the heat release due to the dilution effect. Except for the control paste, it is clear that an enhancement of the

hydration heat evolution was obtained with adding the NS. Also, the heat flow evolution shows a significant increase in the heat liberation in the GP paste as the NS content increased. These results verify that the addition of NS could promote the hydration of the GP blended paste. The increase in the heat of hydration in the early ages was mainly related to the acceleration of the hydration of C_3S and subsequent pozzolanic reaction between the NS and CH [50,51]. NS might play several roles in the hydration acceleration:

(i) the silica with nano-sized particle could become nucleation sites, which was conducive to the precipitation of C-S-H gel and portlandite;
(ii) the NS-CH reaction yielded additional C-S-H gel that acted as a seed for benefiting more gel formation;
(iii) the pozzolanic reaction induced by NS reduced the concentration of Ca^{2+} ions in the solution, leading to re-dissolution of C_3S；
(iv) the absorption of sulfate ions by the large amount of C-S-H due to the acceleration and pozzolanic effects of NS resulted in an acceleration formation of AFm phases.

Consequently, based on the above positive effects, the GP paste modified by NS contributed to greater total heat outputs as compared to the cement paste with only GP. In addition, it is worth pointing out that these positive effects were mainly related to the formation of cement hydration products, which were the major strength contributing constituent of the mortar. Thereby, it is believed that the total hydration heat liberated may correlate strongly with the increased strength. Fig. 10 demonstrates the relationship between the cumulative hydration heat and the corresponding compressive strength. It is surprising to note that the obtained correlations between the heat of hydration of cement paste and the corresponding compressive strength of mortar were fairly good in both 1 day and 3 days, indicating that the hydration process of the cement paste had some important impacts on the strength of the mortar. This increase in the heat output with increasing NS content is thought to cause an enhancement of the mechanical property for the mortar prepared with GP. Indeed, comparing the cumulative heat evolved of 1 day and 3 days, it can be observed that the higher hydration heats in 3-day corresponded to the higher strengths, while for 1-day, the lower hydration heats matched the lower strengths.

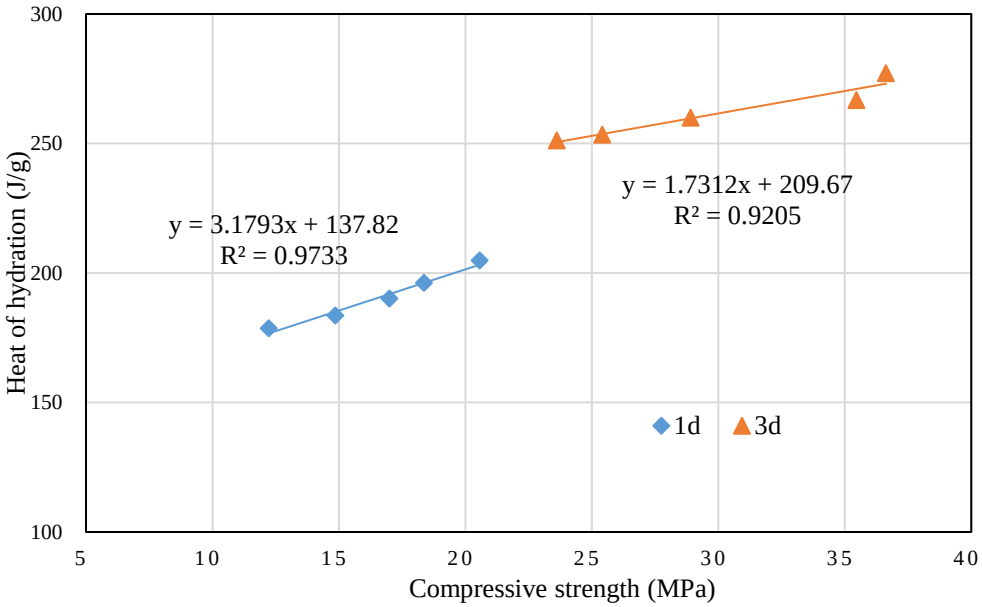

Fig. 10 Relationship between the hydration heat and the compressive strength

4.2 Morphology observation (SEM)

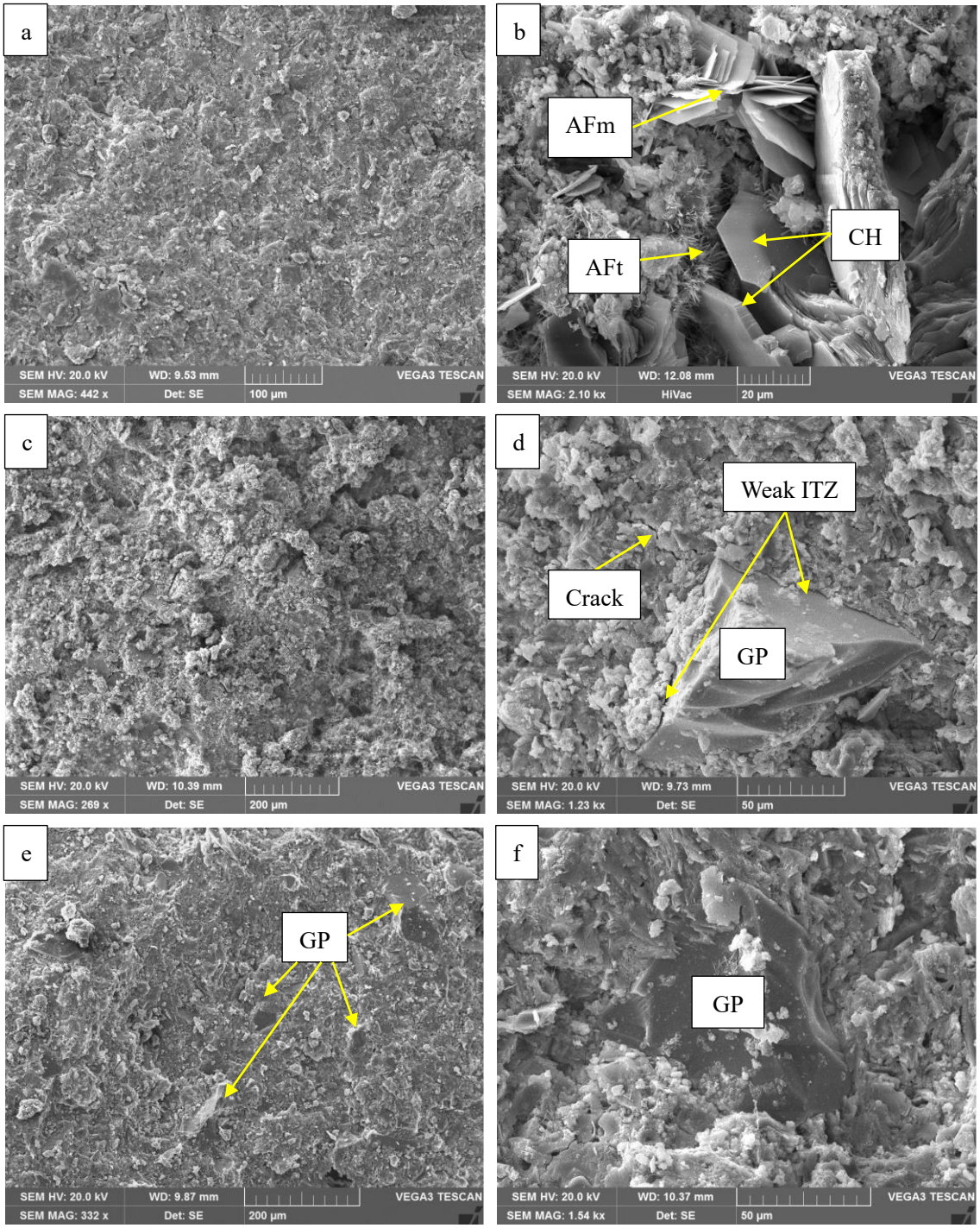

Fig. 11 SEM images of cement pastes at 3 days of curing: (a,b) Control paste; (c,d) GP blended paste without NS; (e,f) GP blended paste with 2% NS

Fig. 11 shows the morphology of the control cement paste and GP blended pastes with and without NS. For the control paste (Fig.11a), a dense matrix was observed as a consequence of high degree of cement hydration. At a close examination of the hydration products (Fig.11b), it can be found that CH with large prismatic shape and the needle-shaped crystals that calcium trisulfoaluminate hydrate (AFt phase) were present. As mentioned, the cement used in this study was a white Portland cement with a high-C_3A content, thus the unstable ettringite would be transformed to monosulfoaluminate hydrates (AFm phase), which had a

thin hexagonal-plate morphology [52]. This is coherent with the observation found in Fig. 11b, demonstrating that layered AFm crystals (hexagonal platelet structure) coexisted with ettringite crystallizes (needle-like crystals).

When the GP was used to replace cement, the structure of the matrix became rougher and the hydration products were less homogenous (see Fig.11c). From Fig.11d, an unreacted GP was identified in the hydrated cement matrix, which indicates that the GP did not exhibit the pozzolanic characteristic at early age. On the contrary, there are cracks present in the periphery of GP due to the weak interface transition zone (ITZ) between the GP and the hydrated products. It is believed that the smooth surface of GP resulted in the weak ITZ. Therefore, the less dense matrix and micro cracks might be responsible for the reduction in the compressive strength as the cement was replaced by GP.

However, in the case of GP paste modified by 2% NS, the microstructure of the hardened specimen was more uniform, compact, and dense similar to the structure of the control specimen (Fig.11e). Although some unreacted GP particles were observed, the inert GP particles were more tightly held in the GP paste matrix containing NS. The dense microstructure is consistent with the previous analysis, which revealed that the addition of NS could promote the C-S-H gel nucleation and densification. Furthermore, based on the pore filling effect, the NS particles might also fill the pores due to their nano-size [53]. Another reason may be due to the fact that the fine NS particles would react with CH around the GP particles to form C-S-H, thus densified the ITZ and improved the weak link between the GP and the binder matrix (see Fig.11f). The NS contributed to the early pozzolanic reaction than GP due to its higher surface area and extremely small particle size. The improvement of ITZ was usually observed in the case of concrete including aggregates and SCMs because of the pozzolanic reaction [54]. However, in this study, the GP also acted as a micro-aggregate since it almost cannot react with water and CH at the early stage. Moreover, the particle size of GP was larger than that of cement. Thus, it was prone to form a weak ITZ in the vicinity of the coarser GP particles. Therefore, it is reasonable to believe that the introduction of fine NS could improve the ITZ similar to the roles of SCMs in concrete. As a result, the addition of NS into the mix prepared with GP was able to densify the microstructure of the cement paste blended with GP and improve the interface of the GP particles in the matrix. The improvement of microstructure was beneficial in enhancing the mechanical strength of the GP blended mix. Also, this will be further verified by the pore structure characteristics presented in section 4.4.

4.3 Thermal gravimetric (TG) analysis

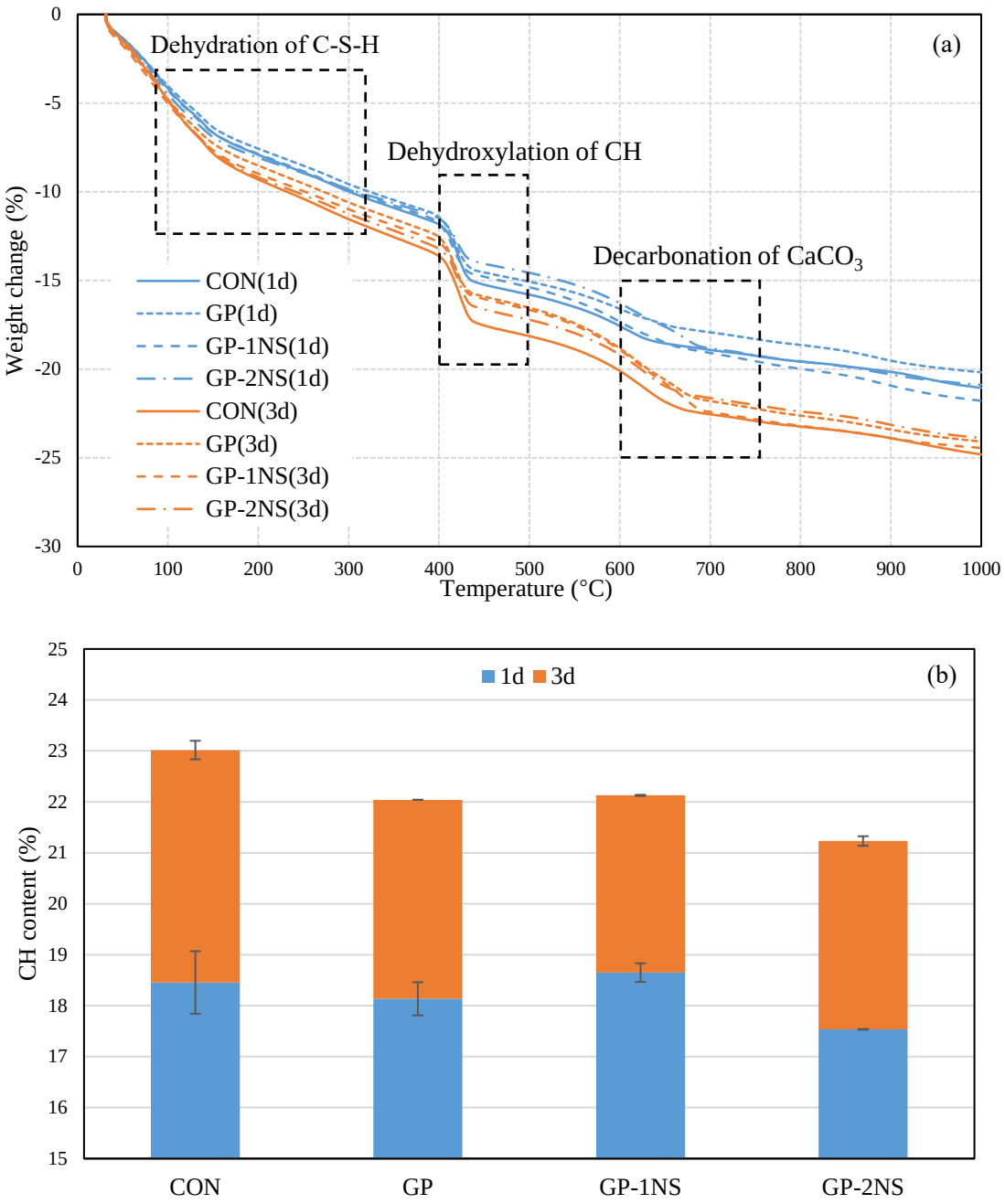

Fig. 12 Thermal calorimetry of cement pastes containing GP and NS: (a) TG weight loss curves; (b) calcium hydroxide content

TG analysis was carried out for the control cement paste, the GP blended paste and the GP paste modified with 1%, 2% NS incorporation after 1 day and 3 days of hydration. The TG results for each mix at different ages are plotted in Fig. 12a. Three main weight losses are visible in the TG curves (the dashed boxes). The first significant loss in weight was due to the release of water unbounded and bounded within the C-S-H, AFt and AFm phases. For temperature around 450 ºC, the CH decomposed to form calcium oxide because of dehydroxylation. The weight loss around 650 ºC corresponded to the decarbonation of $CaCO_3$. Obviously, the weight losses for the specimen at 3 days of curing were greater than that of the specimen at 1 day of

curing since the amount of hydrated products increased with hydration time.

Fig. 12b shows the CH contents of the control cement paste, and the GP pastes with and without NS. Through comparing the CH contents of the control paste and the GP paste, it can be seen that, when 20% of cement was replaced by GP, the CH content of the GP blended mix was higher than 80% of CH content of the plain cement paste regardless of the ages. This indicates that the amount of CH formed was not only dependent on the dilution effect. As observed in section 4.2, the GP generally had limited reactivity at early stage so that the reason due to the consumption of CH by the pozzolanic reaction was excluded. Considering the negligible water absorption of GP, the replacement of cement by GP would increase the effective *w*/*c* ratio, which resulted in an enhancement of the degree of cement hydration at a certain age, thus generating more CH. Therefore, this promotion of hydration compensated the reduction of CH content attributed to the diluted cement.

It is known that CH could be consumed by reacting with NS to form the C-S-H gel. However, as 1% of NS was added into the GP blended mix, the amount of CH was increased instead of decreased. In the case of the cement paste with NS, the CH content was a balance of two effects: (i) the fine NS particles could act as nucleation sites to accelerate the hydration of cement, which released more CH; (ii) the pozzolanic reaction of NS consumed CH. Since the dosage of NS was small (1%), the former effect is believed to control the amount of CH. If the GP blended paste contained a larger amount of NS (2%), the reduced CH content was observed, which indicated that the latter effect was dominant. Actually, irrespective of effect (i) or (ii), the addition of NS was beneficial to the development of strength as more C-S-H gel formed. This conclusion is consistent with the increased early-age compressive strength of the GP mortar modified with NS (section 3.4).

4.4 Pore structure (MIP)

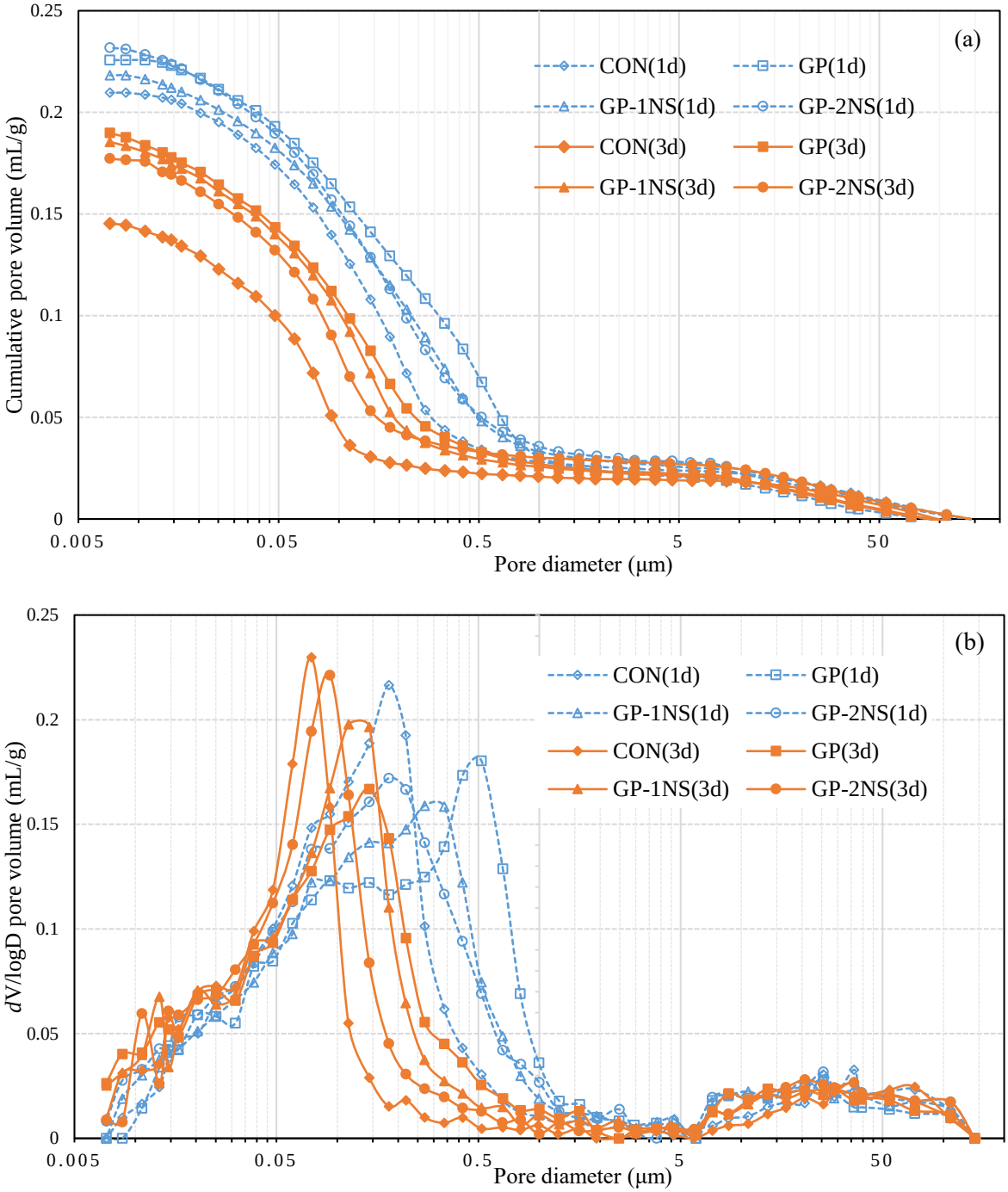

Fig. 13 Pore structure of cement pastes containing GP and NS: (a) cumulative pore volumes; (b) Log-differential volume curve plots

The MIP method was performed to determine the pore volume and the pore size distribution for the cement paste specimens. Fig. 13a gives the cumulative pore volume for the specimens vs. pore diameter. It is obvious that the total intrusion volume decreased with the curing time regardless of the different mixes. This is related to the denser microstructure resulted from the continuous hydration of cement and NS. However, compared to the neat cement paste specimen, the pastes prepared with GP exhibited higher pore volume, which means that the total porosity of the GP blended specimens was higher than that of neat cement paste.

An explanation for this phenomenon is the lesser amount of hydration products formation due to the dilution effect as the cement was replaced by GP. On the other side, the unreacted GP particles in the cement matrix further led to a poor ITZ between the GP and the cement binder matrix (as already stated in section 4.2). This result is also in agreement with a previous work by Lu et al. [19], who stated that a higher effective *w*/*c* due to the inclusion of GP might bring about an increase in porosity of the cement matrix.

When the NS was added in the GP blended paste, the total intruded pore volume was substantially reduced. The reasons are associated with the filling, acceleration and pozzolanic effects of NS addition. The observation had been also verified by the SEM results, i.e. the incorporation of NS could densify the microstructure of the matrix.

Besides porosity, the pore size distribution also plays an important role in determining the strength and permeability of the composite materials [55]. The pore size distribution curves from MIP are shown in Fig. 13b. Apparently, the pore sizes of the specimens after 3 days of curing were smaller than that of the specimens at 1 day of curing, indicating that the structure of the matrix became denser and more compact with time. This is the reason why the samples exhibited improvement in 3-day compressive strength. In spite of the age, the replacement of cement by GP resulted in coarsening of the pore size and the critical pore diameter (the peak value of log differential curve, D_c) shifted towards the right (higher pore size range). This is consistent with the morphology observations (Fig. 11) and the increased porosity results. For the GP blended paste modified with the NS, the incorporation of fine NS shifted the D_c towards smaller sizes and more fine pores were present in comparison with the GP only blended specimen. Moreover, the effect was more pronounced as the dosage of the NS increased. The D_c corresponding to the grouping of the largest fraction of interconnected pores was found to closely influence the ionic diffusion and permeability of cement-based materials [56]. Thus, the reduction in the D_c would probably benefit the transport properties of the GP blended cement paste. Another interesting scenario is that the peaks for the pore size distribution curves tended to be relatively sharper with the content of NS increasing. The above results clearly reveal that the NS in the system contributed to refining the aggravated pore structure induced by the incorporation of GP.

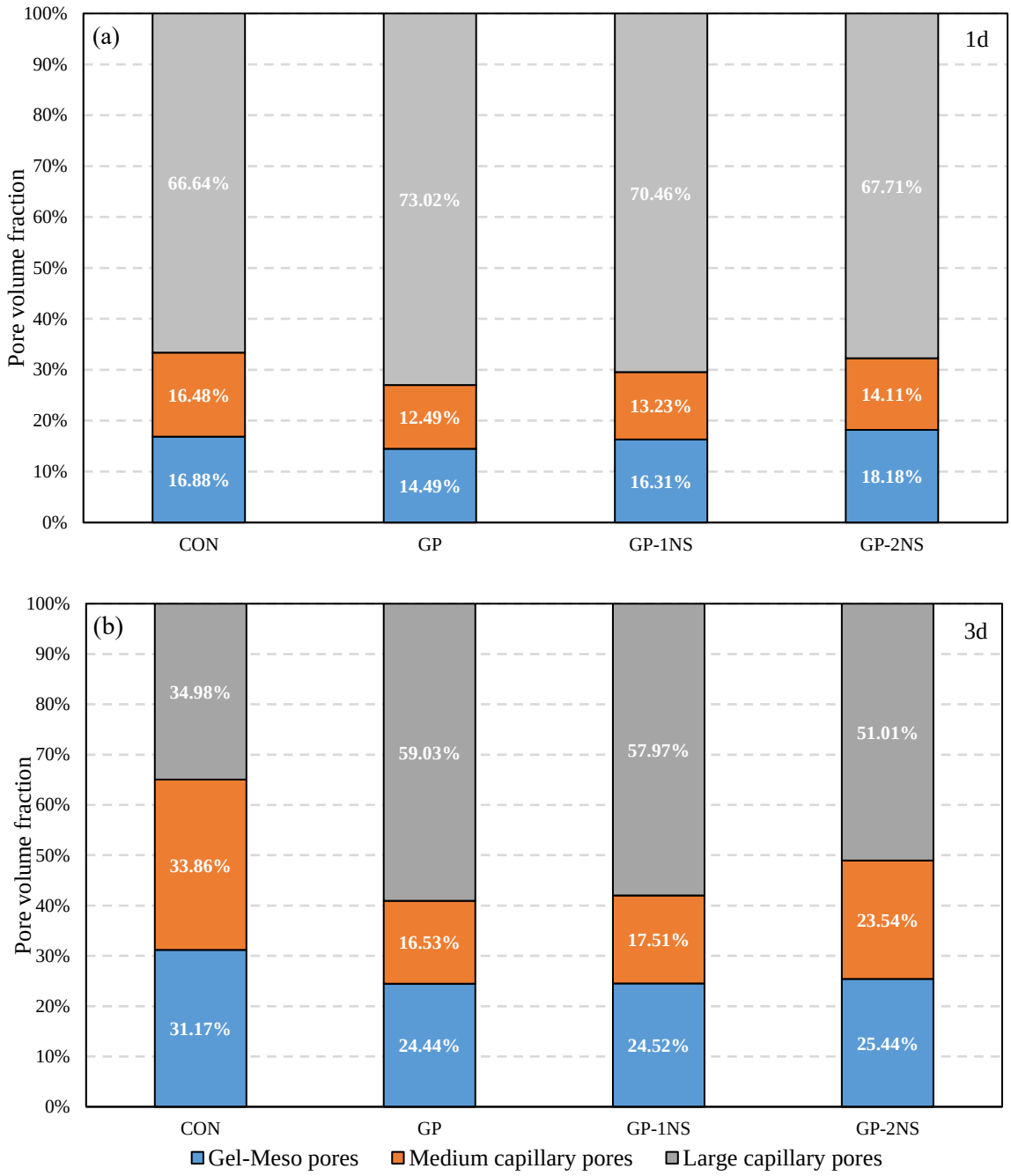

Fig. 14 Pore volume distribution in three size ranges: (a) 1 day of curing; (b) 3 days of curing. Gel-Meso pores: size < 50 nm, medium capillary pores: size from 50 to 100 nm, and large capillary pores: size > 100 nm (size corresponds to diameter). Pore size classification based on [52].

In order to gain more insight into the beneficial effects of NS additions on the pore size refinement for the GP blended mix, the measured pore distribution was divided into three size ranges according to Metha and Monteirio [52]: gel and meso pores (<50 nm), medium capillary pores (50~100 nm) and large capillary pores (>100 nm). The fractions of total pore volume in each specimen at different ages are shown in Fig. 14. It can be found that the inclusion of GP brought about a reduction in the volume of micro and meso-pores and medium capillary pores, while increased the proportion of large capillary pores, especially at 3 days.

The underlying reason lies in the fact that the pore structure was mainly dependent on both how much hydration products were formed and how these products were packed in the mix. On the one side, the replacement of cement by GP reduced the amount of hydration products, i.e. many available voids and space might not be filled. On the other side, as indicated in Fig. 14, the poor GP-paste interface had a definite effect on the pore size distribution.

However, the results also show that with increasing dosage of the NS, the volumes of large capillary pore were decreased whereas the volumes of gel-meso and medium capillary pores were increased. The mechanism of the reduced large capillary porosity in the GP blended paste incorporating NS may be interpreted as physical and chemical effects because of NS addition (as mentioned in Section 3.4). An additional reason can be explained by the improvement of ITZ around the GP particles (Fig. 11), which mitigated the connected path through the pozzolanic reaction with CH.

The above results show the beneficial effects of NS addition on the refinement of pore structure. However, Hou et al. [57] recently reported that addition of nano-sized magnesium oxide decreased the strength and increased the porosity at later ages due to the seeding and coating effects on the surfaces of cement particles. Therefore, the influence of NS incorporation on the performance of glass-based cement mortar at later ages is also needed to be investigated in detail.

4 Conclusion

In this paper, an improved understanding of the effects of nano-sized particles on the early-age properties development was provided which may advance our ability to optimize the components of SCM-containing cementitious materials for optimal performance, both from an engineering perspective and a mechanistic perspective. Although the cost of NS is expensive as compared with construction materials, in this study, less than 2% of the NS addition was enough to significantly improve the early-age properties of the glass-cement mortar containing about 70% glass content (including glass powder and glass aggregates). Based on the experimental results using NS in cement pastes and mortars prepared with glass powder (and glass aggregates), the following conclusions can be drawn:

- The flow values of cement mortar were reduced significantly with increasing dosages of NS. However, in the case of GP mortar modified by NS, the early stiffening was highly dependent on the specific surface area of the NS rather than the effect of NS on the hydration of cement.
- The inclusion of GP delayed the setting times of the cement paste, whereas further addition of NS was conducive to shortening the setting times.
- An encouraging result indicates that the addition of NS could significantly increase the early-age

compressive strength and compensate for the strength losses of the mortar due to the replacement of cement by GP. The increased strength was associated with the physical, acceleration, pozzolanic and pore refinement effects of NS.

- The inclusion of NS in the GP cement paste not only speeded up the initial and acceleration period of hydration but also intensified and shifted the third exothermic peak (AFt to AFm) toward an earlier time. A clear and direct relationship between the heat of hydration and the corresponding early-age compressive strength showed that the increased heat output of the cement paste with increasing NS content was responsible for the enhancement of the mechanical properties of the mortar prepared with GP.
- The use of NS was very advantageous in densifying the microstructure of the GP blended matrix and improving the ITZ between GP particle and binder matrix similar to the roles of SCMs in concrete. The pore structure determination results verified that the NS in the system contributed to refining the coarsening pore size induced by the incorporation of GP.
- This result provides a potential solution for the application of cement-based materials containing much higher volumes of GP or other supplementary cementing materials. Especially, for the calender extrusion method, the addition of a small dosage of NS could not only improve the properties of the glass-cement mortar but also enhance the production efficiency. Therefore, from the points of waste recycling and the efficiency enhancement, the introduction of NS is beneficial.

Acknowledgement

The authors gratefully acknowledge the financial support of The Hong Kong Polytechnic University (Project of Strategic Importance).

References

[1] E.L. Bourhis, Glass: mechanics and technology, Wiley-VCH, Weinheim, 2008.

[2] Environmental Protection Department (EPD). Monitoring of solid waste in Hong Kong (Waste Statistics for 2015): https://www.wastereduction.gov.hk/sites/default/files/msw2015.pdf.

[3] Environment Bureau, Hong Kong Blueprint for Sustainable Use of Resources 2013–2022: http://www.enb.gov.hk/en/files/WastePlan-E.pdf.

[4] A. Mardani-Aghabaglou, M. Tuyan, K. Ramyar, Mechanical and durability performance of concrete incorporating fine recycled concrete and glass aggregates, Mater. Struct. 48 (2015) 2629–2640.

[5] T.C. Ling, C.S. Poon, Spent fluorescent lamp glass as a substitute for fine aggregate in cement mortar, J. Clean. Prod. 161 (2017) 646–654.

[6] M.C. Bignozzi, A. Saccani, L. Barbieri, I. Lancellotti, Glass waste as supplementary cementing materials:

The effects of glass chemical composition, Cem. Concr. Compos. 55 (2015) 45–52.
[7] M. Mirzahosseini, K.A. Riding, Influence of different particle sizes on reactivity of finely ground glass as supplementary cementitious material (SCM), Cem. Concr. Compos. 56 (2015) 95–105.
[8] N.A. Soliman, A. Tagnit-Hamou, Development of ultra-high-performance concrete using glass powder–Towards ecofriendly concrete, Constr. Build. Mater. 125 (2016) 600–612.
[9] A.A. Aliabdo, A.E.M.A. Elmoaty, A.Y. Aboshama, Utilization of waste glass powder in the production of cement and concrete, Constr. Build. Mater. 124 (2016) 866–877.
[10] M. Kamali, A. Ghahremaninezhad, Effect of glass powders on the mechanical and durability properties of cementitious materials, Constr. Build. Mater. 98 (2015) 407–416.
[11] H.J. Du, K.H. Tan, Properties of high volume glass powder concrete, Cem. Concr. Compos. 75 (2017) 22–29.
[12] H. Siad, M. Lachemi, M. Sahmaran, K.M.A. Hossain, Effect of glass powder on sulfuric acid resistance of cementitious materials, Constr. Build. Mater. 113 (2016) 163–173.
[13] A. Omran, A. Tagnit-Hamou, Performance of glass-powder concrete in field applications, Constr. Build. Mater. 109 (2016) 84–95.
[14] A.F. Omran, E. D.-Morin, D. Harbec, A. Tagnit-Hamou, Long-term performance of glass-powder concrete in large-scale field applications, Constr. Build. Mater. 135 (2017) 43–58.
[15] A. Omran, D. Harbec, A. Tagnit-Hamo, R. Gagne, Production of roller-compacted concrete using glass powder: Field study, Constr. Build. Mater. 133 (2017) 450–458.
[16] K. Afshinnia, P.R. Rangaraju, Influence of fineness of ground recycled glass on mitigation of alkali–silica reaction in mortars, Constr. Build. Mater. 81 (2015) 257–267.
[17] K. Afshinnia, P.R. Rangaraju, Impact of combined use of ground glass powder and crushed glass aggregate on selected properties of Portland cement concrete, Constr. Build. Mater. 117 (2016) 263–272.
[18] J.X. Lu, Z.H. Duan, C.S. Poon. Fresh properties of cement pastes or mortars incorporating waste glass powder and cullet, Constr. Build. Mater. 131 (2017) 793–799.
[19] J.X. Lu, Z.H. Duan, C.S. Poon, Combined use of waste glass powder and cullet in architectural mortar, Cem. Concr. Compos. 82 (2017) 34–44.
[20] B. Taha, G. Nounu, Utilizing waste recycled glass as sand/cement replacement in concrete, J. Mater. Civ. Eng. 21(12) (2009) 709–721.
[21] T.C. Ling, C.S. Poon, S.C. Kou, Feasibility of using recycled glass in architectural cement mortars, Cem. Concr. Compos. 33 (2011) 848–854.
[22] T.C. Ling, C.S. Poon, Feasible use of large volumes of GGBS in 100% recycled glass architectural mortar, Cem. Concr. Compos. 53 (2014) 350–356.
[23] S.C. Kou, C.S. Poon, Properties of self-compacting concrete prepared with recycled glass aggregate, Cem. Concr. Compos. 31 (2) (2009) 107–113.
[24] K.H. Tan, H.J. Du, Use of waste glass as sand in mortar: Part I-fresh, mechanical and durability

properties, Cem. Concr. Compos. 35 (2013) 109–117.
[25] H.Y. Wang, A study of the effects of LCD glass sand on the properties of concrete, Waste Management 29 (2009) 335–341.
[26] M.Z. Guo, Z. Chen, T.C. Ling, C.S. Poon, Effects of recycled glass on properties of architectural mortar before and after exposure to elevated temperatures, J. Clean. Prod. 101 (2015) 158–164.
[27] D. Serpa, A. Santos Silva, J. de Brito, J. Pontes, D. Soares, ASR of mortars containing glass, Constr. Build. Mater. 47 (2013) 489–495.
[28] J.X. Lu, B.J. Zhan, Z.H. Duan, C.S. Poon, Improving the performance of architectural mortar containing 100% recycled glass aggregates by using SCMs, Constr. Build. Mater. 153 (2017) 975–985.
[29] F.U.A. Shaikh, S.W.M. Supit, P.K. Sarker, A study on the effect of nano silica on compressive strength of high volume fly ash mortars and concretes, Mater. Des. 60 (2014) 433–442.
[30] M.H. Zhang, J. Islam, Use of nano-silica to reduce setting time and increase early strength of concretes with high volumes of fly ash or slag, Constr. Build. Mater. 29 (2012) 573–580.
[31] P.K. Hou, S. Kawashima, K.J. Wang, D.J. Corr, J.S. Qian, S.P. Shah, Effects of colloidal nanosilica on rheological and mechanical properties of fly ash–cement mortar, Cem. Concr. Compos. 35 (2013) 12–22.
[32] M. Aly, M.S.J. Hashmi, A.G. Olabi, M. Messeiry, E.F. Abadir, A.I. Hussain, Effect of colloidal nano-silica on the mechanical and physical behavior of waste-glass cement mortar, Mater. Des. 33 (2012) 127–135.
[33] P. Sikora, A. Augustyniak, K. Cendrowski, E. Horszczaruk, T. Rucinska, P. Nawrotek, E. Mijowska, Characterization of mechanical and bactericidal properties of cement mortars containing waste glass aggregate and nanomaterials, Mater. 9(8) (2016) 701.
[34] BS EN 1015-3:1999. Methods of test for mortar for masonry—Part 3: Determination of consistence of fresh mortar (by flow table). British Standard Institution; 2007.
[35] ASTM C359-13. Standard test method for early stiffening of hydraulic cement. American Society of Testing Materials; 2014.
[36] BS EN 196-3:2005+A1:2008. Methods of testing cement—Part 3: Determination of setting times and soundness. British Standard Institution; 2009.
[37] K. Scrivener, R. Snellings, B. Lothenbach, A practical guide to microstructure analysis of cementitious materials, CRC Press, New York, USA, 2016.
[38] J.I. Bhatty, K.J. Reid, Use of thermal analysis in the hydration studies of a type 1 Portland cement produced from mineral tailings, Thermochim. Acta. 91 (1985) 95–105.
[39] G.C. Bye, Portland Cement, second ed., Thomas Telford, London, 1999.
[40] M.H. Zhang, J. Islam, S. Peethamparan, Use of nano-silica to increase early strength and reduce setting time of concretes with high volumes of slag, Cem. Concr. Compos. 34 (2012) 650–662.
[41] Y. Chen, Y.F. Deng, M. Li, Influence of nano-SiO_2 on the consistency, setting time, early-age strength, and shrinkage of composite cement pastes, Adv. Mater. Sci. Eng. (2016) 8.

[42] G. Land, D. Stephan, The influence of nano-silica on the hydration of ordinary Portland cement, J. Mater. Sci. 47 (2012) 1011–1017.
[43] V.H. Dodson, Concrete Admixtures, Van Nostrand Reinhold, New York, 1990.
[44] S. Popovics, Concrete-Making Materials, Hemisphere Publishing Corporation, Washington, 1979.
[45] J.W. Bullard, H.M. Jennings, R.A. Livingston, A. Nonat, G.W. Scherer, J.S. Schweitzer, K.L. Scrivener, J.J. Thomas, Mechanisms of cement hydration, Cem. Concr. Res. 41 (2011) 1208–1223.
[46] A. Quennoz, K.L. Scrivener, Interactions between alite and C_3A-gypsum hydrations in model cements, Cem. Concr. Res. 44 (2013) 46–54.
[47] H. Minard, S. Garrault, L. Regnaud, A. Nonat, Mechanisms and parameters controlling the tricalcium aluminate reactivity in the presence of gypsum, Cem. Concr. Res. 37 (2007) 1418–1426.
[48] S. Pourchet, L. Regnaud, J.P. Perez, A. Nonat, Early C_3A hydration in the presence of different kinds of calcium sulfate, Cem. Concr. Res. 39 (2009) 989–996.
[49] A. Quennoz, K.L. Scrivener, Hydration of C_3A–gypsum systems, Cem. Concr. Res. 42 (2012) 1032–1041.
[50] J. Björnström, A. Martinelli, A. Matic, L. Börjesson, I. Panas. Accelerating effects of colloidal nano-silica for beneficial calcium–silicate–hydrate formation in cement, Chem. Phys. Lett. 392 (2004) 242–248.
[51] I.F. Sáez del Bosque, M. Martín-Pastor, S. Martínez-Ramírez, M.T. Blanco-Varela, Effect of temperature on C_3S and C_3S + nanosilica hydration and C-S-H structure, J. Am. Ceram. Soc. 96(3) (2013) 957–965.
[52] P.K. Mehta, P.J.M. Monteiro, Concrete: microstructure, properties, and materials, McGraw-Hill Publishing, London, 2006.
[53] A. Hanif, P. Parthasarathy, H.Y. Ma, T.Y. Fan, Z.J. Li, Properties improvement of fly ash cenosphere modified cement pastes using nano silica, Cem. Concr. Compos. 81 (2017) 35–48.
[54] P. Duan, Z.H. Shui, W. Chen, C.H. Shen, Effects of metakaolin, silica fume and slag on pore structure, interfacial transition zone and compressive strength of concrete, Constr. Build. Mater. 44 (2013) 1–6.
[55] A.M. Brandt. Cement-based composites: materials, mechanical properties and performance (2nd ed). Taylor & Francis, New York, 2009.
[56] P. Halamickova, R.J. Detwiler, D.P. Bentz, E.J. Garboczi, Water permeability and chloride ion diffusion in Portland cement mortars: relationship to sand content and critical pore diameter, Cem. Concr. Res. 25 (1995) 790–802.
[57] P.K. Hou, Y.M. Cai, X. Cheng, X.Z. Zhang, Z.H. Zhou, Z.M. Ye, L.N. Zhang, W.G. Li, S.P. Shah, Effects of the hydration reactivity of ultrafine magnesium oxide on cement-based materials, Mag. Concr. Res. 69 (22) (2017) 1135-1145.